

1966

The crystal structure determination of $[\pi]$ - $C_5H_5Fe(CO)_2Mn(CO)_5$

Peter Jacob Hansen
Iowa State University

Follow this and additional works at: <https://lib.dr.iastate.edu/rtd>

 Part of the [Physical Chemistry Commons](#)

Recommended Citation

Hansen, Peter Jacob, "The crystal structure determination of $[\pi]$ - $C_5H_5Fe(CO)_2Mn(CO)_5$ " (1966). *Retrospective Theses and Dissertations*. 5314.
<https://lib.dr.iastate.edu/rtd/5314>

This Dissertation is brought to you for free and open access by the Iowa State University Capstones, Theses and Dissertations at Iowa State University Digital Repository. It has been accepted for inclusion in Retrospective Theses and Dissertations by an authorized administrator of Iowa State University Digital Repository. For more information, please contact digirep@iastate.edu.

**This dissertation has been
microfilmed exactly as received**

67-2072

**HANSEN, Peter Jacob, 1939-
THE CRYSTAL STRUCTURE DETERMINATION OF
 π -C₅H₅Fe(CO)₂Mn(CO)₅.**

**Iowa State University of Science and Technology, Ph.D., 1966
Chemistry, physical**

University Microfilms, Inc., Ann Arbor, Michigan

THE CRYSTAL STRUCTURE DETERMINATION OF π -C₅H₅Fe(CO)₂Mn(CO)₅

by

Peter Jacob Hansen

A Dissertation Submitted to the
Graduate Faculty in Partial Fulfillment of
The Requirements for the Degree of
DOCTOR OF PHILOSOPHY

Major Subject: Physical Chemistry

Approved:

Signature was redacted for privacy.

In Charge of Major Work

Signature was redacted for privacy.

Head of Major Department

Signature was redacted for privacy.

Dean of Graduate College

Iowa State University
Of Science and Technology
Ames, Iowa

1966

TABLE OF CONTENTS

	Page
INTRODUCTION	1
PREPARATION OF CRYSTALS AND PRELIMINARY X-RAY WORK	3
STRUCTURE DETERMINATION	16
DISCUSSION	19
LITERATURE CITED	45
APPENDIX A	48
APPENDIX B	58

INTRODUCTION

Although the first transition metal carbonyls were prepared, isolated and to a certain extent characterized prior to the turn of the century (1,2), not until 1960 was a carbonyl complex containing two different transition metals prepared and investigated (3). And although the preparation of numerous compounds of this type have since been reported, e.g. $C_5H_5Mo(CO)_3W(CO)_3C_5H_5$ (3), $HFeCo_3(CO)_{12}$ (4), $C_5H_5(CO)-Fe(CO)_2NiC_5H_5$ (5), $C_5H_5(CO)_2FeMo(CO)_3C_5H_5$ (6) and $C_5H_5(CO)Fe(CO)_2Co(CO)_3$ (7), very little structural work has been carried out in this area.

The molecular structure of π -cyclopentadienyliron-manganese heptacarbonyl (hereafter referred to as CIMH) first became of interest because some uncertainty existed as to just how the iron and manganese moieties were bonded to each other. One might consider CIMH to be the adduct of the monomers of $[\pi-C_5H_5Fe(CO)_2]_2$ and $[Mn(CO)_5]_2$, but interestingly enough, these two dimeric compounds contain quite different structural features regarding their metal-metal bonds. The structure of $[\pi-C_5H_5Fe(CO)_2]_2$ was found by Mills (8) to contain two bridging carbonyls and a rather short iron-iron bond length of 2.49 $\overset{\circ}{\text{A}}$ while $[Mn(CO)_5]_2$ was found by Dahl and Rundle (9) to contain no bridging carbonyls and a long Mn-Mn bond length of 2.92 $\overset{\circ}{\text{A}}$. And in addition, although one frequently finds that in metal carbonyl complexes the metal atoms generally attain the effective atomic number of the next noble gas, such an assumption in the case of CIMH fails to exclude either a bridging structure such as that of $[\pi-C_5H_5Fe(CO)_2]_2$ or a structure such as that of $[Mn(CO)_5]_2$ with no bridging carbonyls.

Furthermore, although from steric considerations alone one might have expected the bridging structure, the infrared spectrum of CIMH tended to indicate that this was not the case (6).

PREPARATION OF CRYSTALS AND PRELIMINARY X-RAY WORK

The sample of CIMH which was used in this investigation was prepared by King, Treichel and Stone (6). The preparation was carried out by stirring a pentane solution of $\text{NaMn}(\text{CO})_5$ and $\pi\text{-C}_5\text{H}_5\text{Fe}(\text{CO})_2\text{I}$ for a period of two days. Chromatographic separation yielded the desired product, CIMH, together with the two dimers $[\text{Mn}(\text{CO})_5]_2$ and $[\pi\text{-C}_5\text{H}_5\text{Fe}(\text{CO})_2]_2$.

Single crystals were obtained in this laboratory by vacuum sublimation in a sealed pyrex tubing at about 40°C . The substance readily sublimed at this temperature to produce well-formed single crystals. Although the crystals slowly decompose in air, the rate was sufficiently slow to permit the removal of the crystals to be carried out in the open. Single crystals were still quite difficult to obtain owing to their brittleness and the tenacity with which they adhered to the surface of the glass tubing; however, several single crystals were obtained and their examination under a polarizing microscope indicated that they probably were of quite high quality. The crystal judged most suited for intensity work (owing to its size, shape and well formed faces) was carefully measured using a filar micrometer in order that a crystal absorption correction might later be made. The crystals were mounted and sealed in thin-walled Lindemann glass capillaries since their instability precluded their being mounted on glass fibers.

The alignment of one of the crystal's principal axes parallel to the spindle axis (which is necessary for oscillation and equi-inclination Weissenberg pictures) was quite simply accomplished since the crystals in general possessed one rather long dimension which fortunately also

corresponded to the direction of one of the principal axes. This elongated dimension invariably assumed a position parallel to the capillary walls and quite good alignment was thus obtained merely by using the optical goniometer. In general, a line-up photo would reveal the need for only minor angular corrections. An oscillation picture together with a zero-layer and several upper-layer equi-inclination Weissenberg pictures were obtained.

The Weissenberg photos clearly indicated that the Laue-symmetry was monoclinic and that the axis parallel to the spindle was not the unique axis. Since it was not possible to obtain the monoclinic angle from these Weissenberg photos, the crystal was transferred to the precession camera, a spindle search was initiated, the zone containing the monoclinic angle was located, and zero-, first- and second-layer precession pictures were taken. The Weissenberg and precession pictures were indexed and the following approximate lattice constants and conditions for systematic extinction were obtained:

$$\begin{array}{ll}
 a = 7.23 \text{ \AA} & hk\ell: \text{ no conditions} \\
 b = 33.5 \text{ \AA} & hk0: k = 2n + 1 \\
 c = 12.5 \text{ \AA} & 00\ell: \ell = 2n + 1 \\
 \gamma = 115^\circ &
 \end{array}$$

The systematic extinctions uniquely determined the space group as $P2_1/b$ (No. 14, 1st setting International Tables (10)). The first setting (c-axis unique) was chosen rather than the second setting (b-axis unique) owing to the author's desire to remain consistent with the universally accepted choice of unique axis for all of the other crystal systems.

Using TRACER, a Fortran lattice transformation and cell reduction program (11), it was discovered that the original choice of unit cell was not in line with presently accepted conventions, in that a unit cell could be chosen with a monoclinic angle much closer to ninety degrees. This new unit cell corresponds to what is commonly called the reduced cell. The relationship between the original unit cell and this more conventional reduced cell is given by the following set of axes transformations:

$$\vec{A} = -\vec{a}$$

$$\vec{B} = 2\vec{a} - \vec{b}$$

$$\vec{C} = -\vec{c}$$

(Note: the lower case letters refer to the cell parameters of the original unit cell and the upper case letters to the parameters of the reduced or new cell.)

Although it became necessary to reindex the films due to this change in unit cells, the extinction conditions and space group remained the same. Throughout the remainder of this thesis, all references to lattice parameters or indices refer to those of the reduced cell. From precision measurements using a General Electric single crystal orienter and LCR-2, a Fortran lattice constant refinement program (12), the following lattice parameters were obtained:

$$a = 7.220 \pm 0.006 \text{ \AA}$$

$$b = 30.387 \pm 0.008 \text{ \AA}$$

$$c = 12.498 \pm 0.002 \text{ \AA}$$

$$\gamma = 90.21 \pm 0.10^\circ$$

By the flotation method, using an aqueous solution of ZnCl_2 and a Westphal balance the density of the CIMH crystals was found to be 1.78 gm/cc. This compared quite favorably with a calculated density of 1.80 gm/cc based on eight molecules per unit cell.

Within a 2θ sphere of approximately 145° , complete three dimensional X-ray diffraction intensity data were taken using a General Electric XRD-5 X-ray unit equipped with a goniostat and scintillation counter. The intensity measurements were made using a moving crystal-moving counter technique (i.e. θ - 2θ coupling) with a one hundred second scan covering 3.33° in 2θ and a takeoff angle of 3.0° . Individual background measurements were made for each reflection by repeating the above mentioned scan, but with an ω -offset of 1.8° . Chromium radiation was used with a vanadium foil filter. Other more commonly used radiations were considered unacceptable due to a large absorption coefficient (as in the case of copper radiation) or insufficient peak separation (as in the case of molybdenum radiation).

The raw intensities which were obtained were corrected for Lorentz and polarization factors, crystal and capillary absorption, and crystal decomposition. The crystal absorption correction was made using an absorption correction program for polyhedral crystals adapted from one originally written by Wehe, Busing and Levy (13). The crystal from which the intensity data were measured was a polyhedron having ten faces and fifteen vertices, and the general overall dimensions of $0.23 \times 0.10 \times 0.16$ mm. The linear absorption coefficient (μ) of CIMH for chromium radiation is 83.9cm^{-1} . This value was obtained using the following expression:

$$\mu = (n/V_c) \sum_i (\mu_a)_i$$

where n , is the number of molecules in the unit cell of volume V_c , and the μ_a are atomic absorption coefficients. The crystal transmission factors varied from 29% to 54%.

The capillary absorption correction was made using the following expression derived by Dahm¹:

$$I = I_0 \exp(-\mu t_0 / \cos \sin^{-1}(\sin \theta \sin \chi)).$$

This expression represents an approximation based on the assumption that the X-ray beam rather than passing through a cylindrical glass capillary, passes through two glass plates both of which have the same thickness as the capillary walls, and both of which are tangent to the surface of the capillary, one at the point where the incident beam enters the capillary and the second where the diffracted beam passes out of the capillary. Assuming such a model made the correction much simpler and yet the error which was introduced is thought to have been quite small. The linear absorption coefficient of Lindemann glass for chromium radiation is 47.8 cm^{-1} (14) and the thickness of the capillary walls was measured to be $0.0015 \pm 0.0005 \text{ cm}$. The capillary transmission factors of those reflections included in the refinement varied from 79% to 87%.

Some difficulty was encountered in making the correction for crystal decomposition. It was originally planned that the intensities of three

¹Dahm, D. J. Department of Chemistry, Iowa State University of Science and Technology, Ames, Iowa. Capillary absorption correction. Private communication. 1964.

prominent reflections (hereafter referred to as standards) would be measured repeatedly throughout the period during which the data were collected (approximately five weeks). The intensities of these standards would then provide a measure of both crystal decomposition and instrumental variation, such that the intensities could all be placed on the same scale. Based on the experiences of other members of the research group, it was decided that there would be no need to make repeated measurements of the background count for each of the standards, since the background for a particular reflection generally remains constant. However, about midway through the data collection it was discovered that the background count of the standards had not remained constant, but had increased significantly (presumably due primarily to an increase in electronic "noise"). Thus for the remainder of the period the background count of each standard was measured immediately following the measurement of each peak count. Since the intensities of the standards obtained while the first portion of the data were collected were now known to be somewhat in error, another means of scaling these data had to be employed. The method which was devised consisted in the remeasurement of the intensity of approximately every tenth reflection. (In order to reduce statistical counting errors, the reflections which were chosen were those having rather large intensities.) The ratio of the two measurements of the intensity thus made possible the necessary scaling.

In addition to applying these various corrections to the intensities, their estimated standard deviations (σ_I) were computed, as were the observed structure factors (F_{obs}) and their estimated standard deviations (σ_F). The σ_I were computed using an expression of the following form:

$$\sigma_I^2 = \sum (\partial I / \partial x_i)^2 \sigma_{x_i}^2$$

where the independent variables (x_i) corresponded to the peak count, background count, crystal transmission factor, capillary transmission factor and the decomposition correction factor; and the σ_{x_i} corresponded to their associated standard deviations. The use of this expression assumes that the errors in the independent variables were independent and although strictly speaking this may not have been the case, the errors introduced were thought to have been small. (Evidence for the validity of this presumption was later provided by the excellent results obtained from a weighting scheme analysis which followed the completion of the least squares refinement. This analysis will be discussed later in more detail.)

The σ_F 's were calculated from an expression derived using a finite difference method,

$$\sigma_F = (I + \sigma_I)^{\frac{1}{2}} - I^{\frac{1}{2}}.$$

(Note: The expression in this form, assumes that the intensities have previously been corrected for Lorentz and polarization effects.)

Although σ_I and σ_F are more exactly related by the following expression:

$$\sigma_F = \sigma_I / 2I^{\frac{1}{2}},$$

the former expression was used since at this point it was believed that "unobserved data" would be included in the refinement and the use of the latter expression would have created difficulties in the region of zero intensity. Furthermore, it can be shown through the use of a binomial

expansion that the two expressions are virtually equivalent providing that $I^2 > \sigma_I^2$ (which is generally true except for "unobserved data").

Although the intensities of 1792 reflections were recorded, only 1201 of these were included in the subsequent structure computations and refinement. The difference between these two figures represents intensities which were not included because they were thought to be significantly in error, because their contribution to the solution and refinement was considered to be of dubious value, or because their inclusion did not appear to justify the added expenditure of computer time. These criteria are discussed in somewhat greater detail below.

One source of error was what is commonly called "streak" or more precisely, the diffraction of the noncharacteristic radiation. Although it is highly desirable to have a purely monochromatic X-ray source, in practice this is quite difficult to obtain.

Therefore the diffracted beam which is measured is composed not only of the desired K_α radiation, but also noncharacteristic radiation which is diffracted by higher or lower order reflections. Theoretically the greatest intensity of characteristic radiation relative to noncharacteristic radiation is obtained when V/V_0 equals approximately four, where V is the applied potential to the X-ray tube and V_0 is the excitation potential for the characteristic radiation desired (14).

As an example, for copper and molybdenum targets, with K-line excitation voltages of 8.98 and 20.00kV respectively (14), the optimum applied voltages are 35.9 and 80.00kV. Thus when using copper radiation one generally uses an applied voltage in the neighborhood of about 35kV; however, frequently the available power supplies and/or X-ray tubes are

limited to a maximum of 50kV, which prevents one from using the optimum applied voltage of 80kV for molybdenum radiation and, as might be expected, considerable streaking results

Using chromium radiation, as in this investigation, the optimum applied voltage should have been approximately 24kV, corresponding to an excitation voltage of 5.989kV; however, due in part to an oversight and in part to the lack of previous experience with the use of chromium radiation in this laboratory, the applied voltage which was actually used was 50kV. As a result the intensity of the noncharacteristic radiation was somewhat greater than desired. This noncharacteristic radiation was composed primarily of wavelengths shorter than that of the K_{α} -line (evidenced experimentally by diffraction at smaller Bragg angles) in contrast to the case of molybdenum where primarily the longer wave lengths are present. This is to be expected, since an excessive voltage should produce more high energy (low wave length) radiation, and a less than optimum voltage more low energy (long wave length) radiation.

The magnitude of this error was estimated in the following manner: One very intense first order reflection (the 1 2 1) was scanned, beginning at a 2θ value corresponding to radiation of wave length $1/5$ of the K_{α} wave length up to and slightly beyond the 2θ value corresponding to diffraction of the K_{α} radiation. Assuming the distribution of intensities for all reflections to be the same as for the 1 2 1 (with appropriate Lorentz and polarization corrections applied), calculations were made for each of the 1792 reflections for which intensities had been recorded and if the calculations indicated that over 5% of the intensity was due to streak, the reflection was rejected. Using this criterion, 109

reflections were rejected prior to any of the structure computations; however of these, twenty-seven represented duplicate pieces of data such that only eighty-two independent intensities were actually rejected. Based on a structure factor calculation including these data (later during refinement), this criterion appeared to be quite satisfactory.

A second type of error affected only eight reflections, whose intensities were recorded at high values of 2θ and χ . As a result of both of these angles being large, the incident beam was scattered by the " χ -carriage" and the backgrounds were increased enormously. Generally the background count varied from about 1900 to 2500 counts (per 100sec scan), but for these eight reflections the backgrounds ranged from 10,850 to 18,060 counts. The size of these backgrounds cast considerable doubt upon the accuracy of the intensities which were obtained and these reflections were therefore rejected prior to any of the ensuing computations.

A third type of error was discovered only after the crystal structure determination had advanced to the point where there remained little doubt as to the correct model. It was noted that for six reflections, the magnitudes of the observed structure factors, $|F_{\text{obs}}|$, were extremely small, while the magnitudes of the corresponding calculated structure factors, $|F_{\text{calc}}|$, were rather large. Although the source of this error remains conjecture to some extent, it is thought to have been human error, since during the course of the recording of these data, over six thousand angle settings were manually performed and the likelihood of at least a few errors being made surely must have been great. Furthermore such an error would in general result in the recording of an extremely low or zero intensity since it is quite unlikely that the crystal would

be in a position to allow Bragg diffraction.

As previously stated, certain data were excluded from the structure computations and refinement for reasons other than outright error. Of the 1792 intensities recorded 101 represented duplicate pieces of data. (This figure does not include the 27 reflections, previously mentioned, which were also affected by streak error.) In some cases a reflection's intensity was measured twice, whereas in other cases, the intensities of two equivalent reflections were measured. Rather than including each of these reflections twice, the two measurements were averaged and the average was included together with an increased weighting factor, indicating the greater certainty with which the intensity was known.

The largest group of intensities which were not included in the refinement consisted of what are commonly called "unobserveds". A reflection was considered to be an unobserved reflection if its raw net intensity (the intensity uncorrected for decomposition, absorption, etc.) was equal to or less than 130 counts (per 100 second scan) or if no discernable peak was noted on the counting rate chart.

The 130 count figure was decided upon after performing a simple statistical study of those reflections for which negative intensities were obtained. Although negative intensities do not exist theoretically, they are frequently encountered experimentally because the experimental intensity is equal to the difference between a "peak count" and a "background count" both of which are subject to statistical counting error. The statistical study consisted in making a negative intensity distribution curve (i.e. a plot of negative intensity versus frequency of occurrence) and then noting the magnitude of the negative intensity

which corresponded approximately to the value of three standard deviations. It was then assumed that this curve gave a good representation of the negative portion of the distribution curve for those reflections whose intensities were truly zero and that the curve would be symmetrical about zero such that this 3σ value would also be correct for the positive portion of the distribution curve. Although neither of these assumptions is entirely correct, it is believed that the figure obtained (i.e. 130 counts) by this method is certainly better than one chosen on an entirely arbitrary basis (as is frequently the case).

Although it has been stated by some that "when using the counter technique it is unnecessary to distinguish between observed and 'unobserved'" reflections (15), there are several good reasons for not including unobserveds in a least squares refinement. The method of least squares is based on a Gaussian distribution and although strictly speaking counter data follows a Poisson distribution, in practice the two usually differ only slightly and no appreciable error results from assuming the Gaussian distribution. However, in the case of unobserved data, this assumption is a very poor one for the error distribution differs radically from that of a Gaussian. One reason for this is that the previously mentioned negative intensities which may arise experimentally are in general discarded or replaced by zero intensities. Thus for the extremely small or zero intensities the corresponding distribution curve is truncated (i.e. part or all of the negative portion is missing).

Furthermore, since the least squares weighting factors are equal to the reciprocal of the σ_F^2 , it can be seen from the more exact expression for σ_F given previously that the weighting factors for these

small intensities are either extremely small or zero and thus there is really very little reason to include them in the least squares refinement.

Some workers, believing that unobserved data should be included in the refinement (with non-zero weights) have circumvented this mathematical expression and have assigned a constant weighting factor to all reflections for which $|F_{\text{obs}}| < F_{\text{lim}}$ (where F_{lim} represents some empirical limit); however according to Vand and Dunning (16) such a weighting scheme corresponds to "a rectangular distribution of probabilities" which again differs drastically from a Gaussian distribution and "if this fact is neglected, LS (least squares) can give significantly incorrect results." This was experimentally demonstrated by these authors in the refinement of n-hexatriacontane.

STRUCTURE DETERMINATION

The presence of eight molecules in a unit cell with space group symmetry of order four requires two crystallographically independent molecules. There being one manganese, one iron, twelve carbon and seven oxygen atoms per molecule, the structure therefore contains 126 independent positional parameters (neglecting hydrogen atoms). In addition to the positional parameters, the refinement included six anisotropic temperature factors for each heavy atom (iron or manganese), one isotropic temperature factor for each light atom (carbon or oxygen) and a scale factor which placed the observed structure factors on an absolute scale. The structure determination thus consisted in the solution of a 189 variable problem.

A Patterson map was computed from the observed structure factors which were "sharpened" using the method of Jacobson, Wunderlich and Lipscomb (17) as programmed by Barry Granoff.¹ From an analysis of the Harker sections of this "sharpened" Patterson map, the positions of two of the heavy atoms were obtained. Using these two atoms to determine the signs, an electron density map was computed which revealed the positions of the two remaining heavy atoms in the asymmetric unit. The positions of the twelve Harker and twenty-four non-Harker peaks corresponding to these four heavy atoms were subsequently verified on the Patterson map. (An interesting side light concerns the initial attempts to obtain the positions of all four heavy atoms directly from the Patterson map.

¹Granoff, B. Department of Chemistry, Iowa State University of Science and Technology, Ames, Iowa. Patterson sharpening program. Private communication. 1964.

At one point, it was believed that the positions of three of the heavy atoms were known, however repeated attempts to locate the fourth only met with failure. It was then discovered that the position of one of the three atoms was erroneous, even though the position was entirely consistent with the positions of eleven peaks on the Patterson map.) The positions of the carbon and oxygen atoms were then obtained by employing conventional "heavy atom" techniques. Four successive electron-density maps were required to locate the thirty-eight light atoms.

At this point, a full matrix least squares refinement was initiated with the four heavy atoms being refined anisotropically and the thirty-eight light atoms being refined isotropically. The computations were performed using the Fitzwater-Benson-Jackobs least squares program¹ on the IBM 7074 computer. The atomic scattering factors used in this refinement were those calculated by Hanson *et al.* (18) from Hartree-Fock-Slater wave functions. During the latter stages of refinement the iron and manganese scattering factors were modified so as to include a correction for anomalous dispersion. The anomalous dispersion correction accounts for the fact that the electrons in the crystal are not free electrons, but are bound electrons whose scattering power may be different and whose scattered wave may have a different phase. An atomic scattering factor may be expressed as

$$f = f_0 - f' - i f''$$

¹Fitzwater, D. R., Benson, J. E., both of Ames Laboratory, Atomic Energy Commission, Ames, Iowa. Jackobs, J. J., (present address) Arizona State University, Tempe, Arizona. Least squares package. Private communication. 1965.

where f_0 is the "ordinary" atomic scattering factor assuming free electrons and f' and f'' are respectively the real and imaginary dispersion corrections. In the case of iron and manganese (with Cr K_{α} radiation) the imaginary corrections are very small and were thus neglected, but the real corrections were considered significant and were applied using the values listed by Dauben and Templeton in the International Tables, Vol. III (14).

Following several cycles of least squares refinement a difference electron density map was computed which revealed some maxima in positions consistent with the locations of the cyclopentadienyl ring hydrogens. The positions of the hydrogens were then calculated, assuming a C-H distance of 1.0 Å and included, although not varied, in the ensuing refinement.

After several additional cycles of full matrix least squares refinement, a final agreement factor ($R = \sum ||F_o| - |F_c|| / \sum |F_o|$) of 0.064 was obtained. Following completion of the refinement, the veracity of the least squares weighting scheme was established by means of a plot of $\omega \Delta^2$ (where $\Delta = ||F_o| - |F_c||$) versus $\sin \theta/\lambda$, the $\omega \Delta^2$ values representing averages over ranges of $\sin \theta/\lambda$. The plot indicated, within experimental error, that $\omega \Delta^2$ was independent of $\sin \theta/\lambda$, which is the desired result.

DISCUSSION

The crystal structure of CIMH consists of discrete molecules and although there are two crystallographically independent molecules, both of them possess essentially the configuration shown in Figure 1. The numbering system used in this figure will be employed throughout the remainder of this discussion and in the tables.

The final heavy atom positional parameters and anisotropic temperature factors together with their standard errors are presented in Table 1, and the final light atom positional parameters and isotropic temperature factors together with their standard errors are presented in Table 2. The positional parameters (or coordinates) are tabulated as fractions of the unit cell edges. The form of the anisotropic temperature factors is

$$\exp(-h^2\beta_{11} - k^2\beta_{22} - l^2\beta_{33} - 2hk\beta_{12} - 2hl\beta_{13} - 2kl\beta_{23})$$

while the form of the isotropic temperature factor is

$$\exp(-B\sin^2\theta/\lambda^2).$$

Table 3 contains a list of the individual interatomic bond distances and their standard errors and also the mean values of chemically equivalent bond lengths. A list of pertinent nonbonded intramolecular distances and their standard errors are given in Table 4, while Table 5 lists the interatomic bond angles together with their associated standard errors.

All of the interatomic distances and angles, and their standard errors contained in these tables were computed using a modified version of the Busing-Martin-Levy ORFFE program (19), which in turn used the

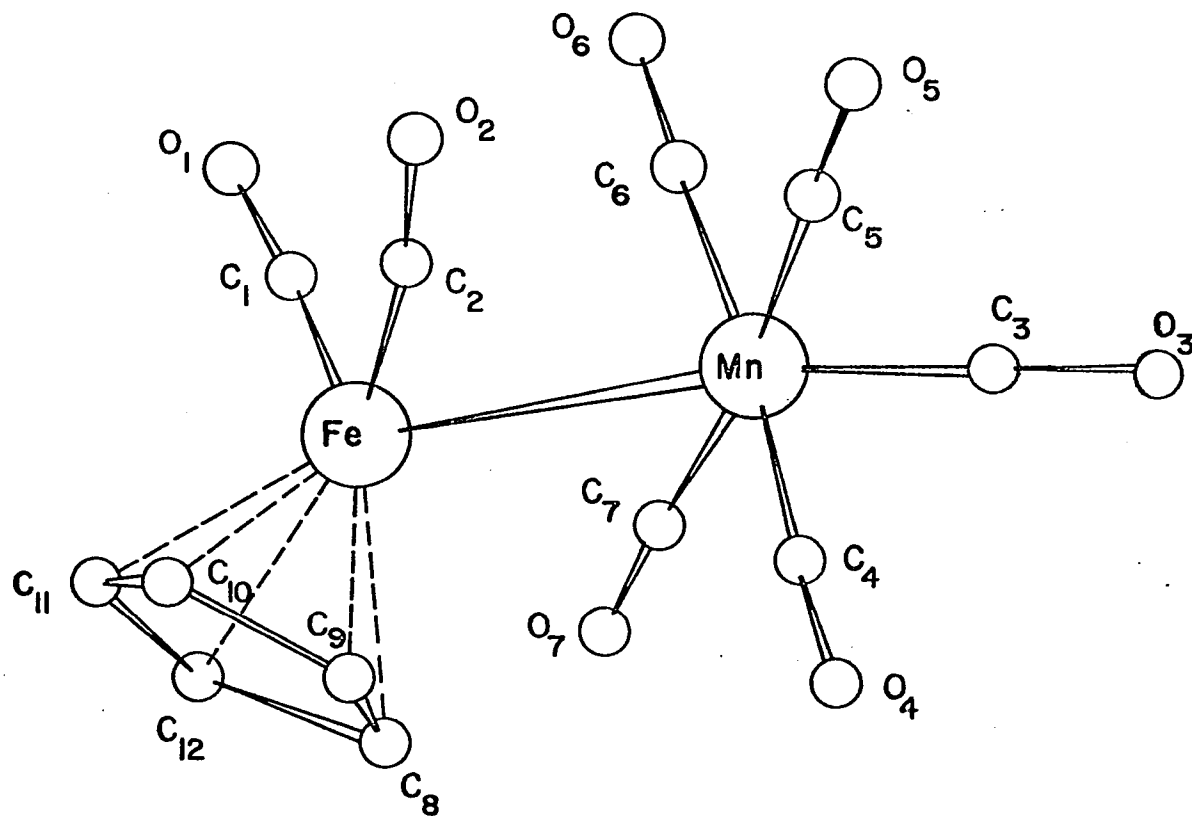


Figure 1. The molecular configuration of $\pi\text{-C}_5\text{H}_5\text{Fe}(\text{CO})_2\text{Mn}(\text{CO})_5$

Table 1. Final heavy atom positional and thermal parameters and their standard errors (β 's are $\times 10^5$)

Atom	x ^a	y	z	β_{11}	β_{22}	β_{33}	β_{12}	β_{13}	β_{23}
<u>Molecule 1</u>									
Fe	0.42112 (41)	0.13605 (8)	0.31602 (21)	2891 (92)	125 (4)	548 (23)	47 (14)	-172 (37)	-24 (7)
Mn	0.35359 (43)	0.22531 (8)	0.37049 (22)	2595 (91)	97 (4)	804 (28)	-67 (14)	-89 (39)	27 (8)
<u>Molecule 2</u>									
Fe	0.07489 (42)	0.02886 (8)	0.75336 (21)	3091 (90)	104 (4)	573 (21)	-78 (13)	59 (37)	-16 (7)
Mn	0.14612 (42)	0.11621 (8)	0.82457 (21)	2458 (90)	104 (4)	565 (23)	-52 (13)	-77 (39)	13 (8)

^aNumbers in parentheses here and in subsequent tables are standard errors in the least significant figures.

Table 2. Final light atom positional and thermal parameters and their standard errors

Atom	x	y	z	B
<u>Molecule 1</u>				
C ₁	0.2891(30)	0.1433(6)	0.2072(16)	7.02(99)
O ₁	0.1758(22)	0.1432(5)	0.1351(12)	8.85(75)
C ₂	0.2344(25)	0.1258(5)	0.4023(13)	4.80(76)
O ₂	0.1213(19)	0.1151(4)	0.4591(10)	6.63(59)
C ₃	0.3538(30)	0.2822(7)	0.3910(17)	8.01(106)
O ₃	0.3503(23)	0.3209(6)	0.4078(13)	10.23(85)
C ₄	0.4511(28)	0.2834(6)	0.9628(14)	6.06(86)
O ₄	0.3336(19)	0.2878(4)	0.0234(11)	7.21(64)
C ₅	0.1999(27)	0.2128(6)	0.4808(15)	6.03(87)
O ₅	0.1012(21)	0.2063(4)	0.5511(12)	8.13(69)
C ₆	0.1526(31)	0.2275(6)	0.2824(16)	6.77(95)
O ₆	0.0252(24)	0.2287(5)	0.2271(12)	9.05(76)
C ₇	0.4927(31)	0.2711(6)	0.7546(18)	7.75(102)
O ₇	0.3968(22)	0.2683(5)	0.6785(13)	9.02(74)
C ₈	0.2850(26)	0.3591(6)	0.8259(15)	6.04(84)
C ₉	0.3511(27)	0.3867(6)	0.9094(14)	6.09(86)
C ₁₀	0.4444(28)	0.4217(6)	0.8580(16)	6.85(93)
C ₁₁	0.4307(29)	0.4152(6)	0.7487(17)	7.15(96)
C ₁₂	0.3339(28)	0.3762(6)	0.7281(15)	7.00(95)
H ₈	0.2139	0.3312	0.8358	5.0
H ₉	0.3362	0.3825	0.9883	5.0
H ₁₀	0.4918	0.0533	0.3954	5.0
H ₁₁	0.4831	0.4353	0.6929	5.0
H ₁₂	0.3056	0.3630	0.6565	5.0

Table 2. (Continued)

Atom	x	y	z	B
<u>Molecule 2</u>				
C ₁	0.2279(27)	0.0135(6)	0.8526(15)	6.05(85)
O ₁	0.3335(19)	0.4997(4)	0.5865(10)	7.30(63)
C ₂	0.2430(28)	0.0384(6)	0.6599(16)	6.33(89)
O ₂	0.3636(22)	0.0411(4)	0.5977(11)	8.28(70)
C ₃	0.1457(25)	0.1699(6)	0.9751(14)	5.90(85)
O ₃	0.1414(20)	0.2066(5)	0.9092(11)	8.53(73)
C ₄	0.0407(28)	0.3731(6)	0.2310(15)	6.25(90)
O ₄	0.1603(20)	0.3655(4)	0.1721(11)	7.75(66)
C ₅	0.3103(28)	0.1296(6)	0.7190(15)	6.46(94)
O ₅	0.4191(22)	0.1388(5)	0.6544(12)	8.73(74)
C ₆	0.3391(26)	0.0996(5)	0.9107(14)	5.14(78)
O ₆	0.4608(20)	0.0910(4)	0.9665(10)	7.19(63)
C ₇	0.0097(26)	0.4043(6)	0.4293(15)	5.69(82)
O ₇	0.1093(19)	0.4168(4)	0.4943(10)	6.88(60)
C ₈	0.2191(28)	0.4656(6)	0.2601(15)	6.77(91)
C ₉	0.1576(28)	0.4736(6)	0.1524(16)	6.85(92)
C ₁₀	0.0663(28)	0.0146(6)	0.3486(16)	7.02(95)
C ₁₁	0.0679(28)	0.0306(6)	0.2446(16)	6.78(90)
C ₁₂	0.1594(29)	0.0007(6)	0.1770(16)	7.35(99)
H ₈	0.2892	0.4396	0.2867	5.0
H ₉	0.1776	0.4542	0.0892	5.0
H ₁₀	0.0088	0.0289	0.4121	5.0
H ₁₁	0.0122	0.0591	0.2218	5.0
H ₁₂	0.8101	0.0036	0.0985	5.0

Table 3. Individual interatomic bond distances and their standard errors together with the mean values of equivalent^a distances (in Å)

Atoms	Molecule 1	Molecule 2	Mean
Mn-Fe	2.840(4)	2.845(4)	
Mn-Fe			2.843
Fe-C ₁	1.676(26)	1.726(24)	
Fe-C ₂	1.754(23)	1.709(25)	
Fe-C ² (carbonyl)			1.716
Mn-C ₃	1.748(28)	1.750(22)	
Mn-C ³ (axial carbonyl)			1.749
Mn-C ₄	1.841(25)	1.815(26)	
Mn-C ₅	1.809(25)	1.819(26)	
Mn-C ₆	1.823(27)	1.833(23)	
Mn-C ₇	1.827(29)	1.833(24)	
Mn-C ⁷ (equatorial carbonyl)			1.825
Fe-C ₈	2.130(23)	2.131(24)	
Fe-C ₉	2.133(22)	2.101(24)	
Fe-C ₁₀	2.077(23)	2.096(23)	
Fe-C ₁₁	2.071(23)	2.078(23)	
Fe-C ₁₂	2.116(24)	2.102(25)	
Fe-C ¹² (ring)			2.104 ^a
C ₁ -O ₁	1.217(25)	1.158(22)	
C ₂ -O ₂	1.129(21)	1.170(24)	
C ² -O ² (Fe)			1.169
C ₃ -O ₃	1.194(27)	1.195(22)	
C ³ -O ³ (Mn, axial)			1.195
C ₄ -O ₄	1.146(23)	1.159(23)	
C ₅ -O ₅	1.148(23)	1.160(24)	
C ₆ -O ₆	1.152(25)	1.153(21)	
C ₇ -O ₇	1.180(26)	1.150(22)	
C ⁷ -O ⁷ (Mn, equatorial)			1.156
C ₈ -C ₉	1.421(27)	1.439(29)	
C ₉ -C ₁₀	1.413(29)	1.410(28)	
C ₁₀ -C ₁₁	1.384(29)	1.388(29)	
C ₁₁ -C ₁₂	1.398(31)	1.407(29)	
C ₁₂ -C ₈	1.374(28)	1.396(29)	
C-C ⁸ (ring)			1.403 ^a

^aAs discussed later, the Fe-C(ring) and C-C(ring) and interatomic distances may not be chemically equivalent.

Table 4. Pertinent nonbonded intramolecular distances and their standard error (in Å)

Atoms	Molecule 1	Molecule 2	Atoms	Molecule 1	Molecule 2
<u>Carbonyl-carbonyl distances</u>					
C ₃ -C ₄	2.60(4)	2.60(3)	C ₄ -C ₅	2.53(4)	2.54(3)
C ₃ -C ₅	2.63(4)	2.59(3)	C ₅ -C ₆	2.54(3)	2.57(3)
C ₃ -C ₆	2.60(4)	2.60(3)	C ₆ -C ₇	2.58(4)	2.53(3)
C ₃ -C ₇	2.60(4)	2.60(3)	C ₇ -C ₄	2.65(4)	2.66(3)
C ₁ -C ₆	2.90(3)	2.83(3)	O ₁ -O ₆	3.04(2)	2.99(2)
C ₂ -C ₅	2.83(3)	2.91(3)	O ₂ -O ₅	3.00(2)	3.08(2)
<u>Carbonyl-ring distances^a</u>					
C ₇ -C ₈	3.20(3)	3.20(3)	C ₇ -C ₁₂	3.41(3)	3.39(3)
O ₇ -C ₈	3.42(3)	3.37(3)	O ₇ -C ₁₂	3.37(3)	3.35(3)
C ₇ -H ₈	2.91	2.90	C ₇ -H ₁₂	3.34	3.27
O ₇ -H ₈	3.05	2.98	O ₇ -H ₁₂	2.97	2.92
C ₄ -C ₈	3.11(3)	3.11(3)	C ₄ -C ₉	3.29(3)	3.31(3)
O ₄ -C ₈	3.30(3)	3.26(3)	O ₄ -C ₉	3.33(3)	3.30(3)
C ₄ -H ₈	2.75	2.79	C ₄ -H ₉	3.14	3.19
O ₄ -H ₈	2.83	2.83	O ₄ -H ₉	2.91	2.89
C ₁ -C ₁₁	2.75(3)	2.80(3)	C ₂ -C ₁₀	2.79(3)	2.75(4)
C ₁ -H ₁₁	2.91	2.95	C ₂ -H ₁₀	2.89	2.88
<u>Metal-carbonyl distances</u>					
Mn-C ₁	3.25(2)	3.20(2)	Mn-C ₂	3.17(2)	3.21(2)
Fe-C ₄	3.19(2)	3.11(2)	Fe-C ₆	3.42(2)	3.48(2)
Fe-C ₅	3.50(2)	3.52(2)	Fe-C ₇	2.99(3)	3.06(2)

^aAs stated in the text, the hydrogen positions were calculated assuming a C-H distance of 1.0 Å. The distances tabulated here which include a hydrogen atom are thus only approximations.

Table 5. Intramolecular bond angles and their standard errors (in degrees)

Atoms	Molecule 1	Molecule 2	Atoms	Molecule 1	Molecule 2
Fe-C ₁ -O ₁	169.5(2.1)	173.5(2.0)	C ₃ -Mn-C ₄	93.0(1.1)	93.6(1.0)
Fe-C ₂ -O ₂	173.1(1.7)	173.9(2.0)	C ₃ -Mn-C ₅	95.4(1.1)	93.2(1.0)
Mn-C ₃ -O ₃	177.9(2.4)	178.6(2.1)	C ₃ -Mn-C ₆	92.9(1.1)	92.8(0.9)
Mn-C ₄ -O ₄	177.1(1.9)	178.6(1.9)	C ₃ -Mn-C ₇	93.3(1.2)	93.2(1.0)
Mn-C ₅ -O ₅	177.8(2.0)	177.6(2.1)	C ₄ -Mn-C ₅	87.8(1.0)	88.7(1.0)
Mn-C ₆ -O ₆	179.6(2.1)	177.2(1.8)	C ₅ -Mn-C ₆	88.9(1.0)	89.5(1.0)
Mn-C ₇ -O ₇	178.5(2.2)	179.1(2.0)	C ₆ -Mn-C ₇	90.1(1.1)	87.3(0.9)
Mn-Fe-C ₁	88.2(0.8)	85.0(0.7)	C ₇ -Mn-C ₄	92.3(1.1)	93.7(1.0)
Mn-Fe-C ₂	83.5(0.6)	86.0(0.7)	C ₄ -Mn-C ₆	173.5(1.0)	173.5(0.9)
Fe-Mn-C ₃	168.6(0.9)	169.2(0.8)	C ₅ -Mn-C ₇	171.2(1.0)	173.0(0.9)
Fe-Mn-C ₄	83.0(0.7)	80.4(0.7)	C ₈ -C ₉ -C ₁₀	105.6(1.9)	107.6(2.0)
Fe-Mn-C ₅	95.1(0.7)	95.6(0.7)	C ₉ -C ₁₀ -C ₁₁	107.8(2.0)	107.4(2.0)
Fe-Mn-C ₆	91.7(0.7)	93.6(0.7)	C ₁₀ -C ₁₁ -C ₁₂	109.8(2.2)	109.8(2.1)
Fe-Mn-C ₇	76.2(0.7)	78.3(0.6)	C ₁₁ -C ₁₂ -C ₈	106.5(2.1)	107.6(2.1)
C ₁ -Fe-C ₂	94.9(1.0)	94.7(1.1)	C ₁₂ -C ₈ -C ₉	110.2(2.0)	107.5(2.0)

variance-covariance matrix of the parameters obtained from the Fitzwater-Benson-Jackobs least squares program.¹ Owing to certain restrictions of the ORFFE program, the variance-covariance matrix was computed with the underlying assumption that the thermal behavior of all of the atoms was isotropic and thus it became necessary to convert the anisotropic temperature factors of the heavy atoms to "equivalent" isotropic temperature factors prior to the computation of the matrix. This conversion was made using the method of Hamilton (20). Although this certainly must have resulted in the introduction of some inaccuracy, hand calculations tended to indicate that the discrepancies are probably quite small and that if anything, the standard errors obtained may have been slightly larger than the true values.

Figure 2 contains a complete list of the observed and calculated structure factors of the 1201 reflections which were included in the least squares refinement.

Although the original purpose behind this crystal structure investigation concerned primarily the means by which the two moieties were bonded together, the results of the investigation have yielded several additional interesting features. These include the structural dissimilarities between the two crystallographically independent molecules, the differences between the $\text{Mn}(\text{CO})_5$ groups found in CIMH and those found in $\text{Mn}_2(\text{CO})_{10}$ and $\text{HMn}(\text{CO})_5$, the nonlinearity of the Fe-C-O groups, and some evidence which

¹Fitzwater, D. R., Benson, J. E., both of Ames Laboratory, Atomic Energy Commission, Ames, Iowa. Jackobs, J. J., (present address) Arizona State University, Tempe, Arizona. Least squares package. Private communication. 1965.

H	K	L	F0BS	FCAL	H	K	L	F0BS	FCAL	H	K	L	F0BS	FCAL	H	K	L	F0BS	FCAL					
5	4	0	31.5	-36.0	-1	17	4	55.0	58.5	-2	13	2	109.7	109.7	-3	11	1	39.4	37.7	-4	18	0	38.6	-35.0
5	8	0	51.5	-51.0	-1	18	4	72.2	-26.4	-2	14	2	72.4	-76.0	-3	11	1	10.1	10.6	-4	18	0	15.0	-30.4
5	10	0	16.0	-16.2	-1	19	4	51.1	-55.0	-2	15	2	21.4	20.4	-3	14	1	64.9	61.5	-4	1	1	14.2	-17.0
5	12	0	20.4	-19.0	-1	20	4	51.7	-51.4	-2	16	2	52.0	52.3	-3	16	1	64.5	61.8	-4	2	1	22.7	-78.2
5	14	0	17.7	-21.7	-1	21	4	46.0	-48.9	-2	19	2	47.5	-49.4	-3	17	1	17.0	-22.3	-4	2	1	25.4	-9.2
5	2	1	116.9	-75.5	-1	23	4	13.9	15.7	-2	20	3	36.4	34.9	-3	18	1	14.1	-15.0	-4	5	1	21.2	-17.4
5	3	1	15.8	33.0	-1	0	5	24.7	-75.8	-2	21	2	39.4	40.3	-3	19	1	12.1	5.8	-4	6	1	45.5	-41.8
5	4	1	72.5	72.5	-1	1	5	62.6	61.5	-2	22	2	12.3	13.1	-3	20	1	13.0	-11.8	-4	7	1	21.0	-15.9
5	5	1	28.7	-26.8	-1	2	5	27.4	-78.7	-2	23	2	24.9	27.1	-3	21	1	29.5	20.1	-4	8	1	45.4	-45.7
5	6	1	30.8	-32.4	-1	3	5	39.1	-39.1	-2	24	2	65.4	65.4	-3	22	1	18.9	13.6	-4	9	1	34.5	34.5
5	7	1	16.1	16.8	-1	4	5	20.3	-17.1	-2	25	2	71.0	211.6	-3	23	1	19.0	-19.6	-4	10	1	36.3	36.6
5	10	1	32.8	-32.6	-1	5	5	13.2	-16.2	-2	3	1	87.3	-84.6	-3	2	2	39.6	-76.2	-4	11	1	10.4	-30.7
5	11	1	21.0	71.7	-1	6	5	42.8	45.7	-2	4	3	62.6	-63.3	-3	4	2	27.0	-21.3	-4	12	1	19.4	17.1
5	12	1	16.6	19.6	-1	7	5	65.1	59.8	-2	5	3	143.7	143.1	-3	5	2	34.5	34.1	-4	13	1	14.8	-17.7
5	14	1	16.1	12.0	-1	8	5	52.4	50.9	-2	6	3	59.6	-54.2	-3	6	2	15.6	-16.4	-4	14	1	51.3	48.0
5	1	2	15.6	-11.6	-1	9	5	23.1	78.7	-2	10	3	17.9	-11.1	-3	7	2	31.4	-28.0	-4	0	2	20.0	4.6
5	2	2	17.5	13.8	-1	12	5	46.9	47.8	-2	11	3	67.0	-61.4	-3	8	2	58.2	-54.4	-4	1	2	38.1	-46.4
5	3	2	20.6	22.3	-1	13	5	18.3	-14.3	-2	12	3	51.6	-46.7	-3	9	2	26.7	-22.4	-4	2	2	25.9	-30.0
5	4	2	26.2	23.7	-1	14	5	19.2	-20.3	-2	13	3	82.3	83.7	-3	10	2	62.4	-57.7	-4	3	2	59.4	-58.1
5	5	2	32.3	34.8	-1	15	5	29.4	24.8	-2	14	3	43.0	-47.8	-3	11	2	36.3	30.9	-4	4	2	25.0	-76.5
5	7	2	26.5	27.7	-1	16	5	50.7	61.1	-2	15	3	28.7	28.7	-3	12	2	10.8	-25.5	-4	5	2	73.0	-74.0
5	8	2	35.6	38.5	-1	17	5	20.1	-24.6	-2	18	3	32.1	-34.7	-3	13	2	40.2	-46.2	-4	6	2	65.7	63.8
5	9	2	35.4	-39.3	-1	18	5	12.4	13.8	-2	19	3	12.4	-38.0	-3	14	2	16.3	-12.7	-4	7	2	38.9	-45.2
5	10	2	12.1	13.5	-1	0	6	51.8	-54.3	-2	20	3	34.3	41.3	-3	15	2	22.3	-20.3	-4	8	2	42.8	-41.9
5	11	2	22.0	21.4	-1	2	6	39.3	37.1	-2	22	3	12.7	-14.3	-3	16	2	14.7	16.6	-4	9	2	17.1	-21.4
5	13	2	10.6	-15.3	-1	4	6	38.3	-41.9	-2	0	4	106.9	116.6	-3	17	2	12.6	12.4	-4	10	2	53.8	-50.7
5	13	3	26.6	-30.7	-1	5	6	88.5	87.2	-2	1	4	17.5	18.2	-3	20	2	36.1	28.8	-4	11	2	29.1	-29.4
5	1	3	40.6	-16.8	-1	6	6	26.2	-27.9	-2	2	4	26.9	29.3	-3	21	2	29.5	-27.5	-4	12	2	23.7	20.0
5	3	3	28.6	31.1	-1	7	6	50.7	-46.5	-2	6	4	103.4	105.4	-3	1	3	84.9	84.6	-4	0	3	49.7	45.4
5	7	3	33.4	35.1	-1	8	6	24.7	-18.1	-2	7	4	17.8	-14.9	-3	2	3	71.3	77.7	-4	3	3	17.6	-25.5
5	8	3	24.6	26.0	-1	10	6	67.5	66.0	-2	8	4	37.6	29.5	-3	3	3	56.5	-60.4	-4	4	3	38.5	38.5
5	8	3	17.2	-17.2	-1	11	6	13.7	13.7	-2	9	4	11.4	13.7	-3	4	3	81.0	79.7	-4	5	3	14.9	4.1
5	10	3	11.5	5.7	-1	12	6	43.8	45.6	-2	11	4	45.6	41.8	-3	5	3	46.0	-38.5	-4	6	3	19.2	16.0
5	11	3	41.2	-41.6	-1	13	6	49.8	49.8	-2	12	4	30.0	-29.4	-3	6	3	117.3	110.5	-4	7	3	18.6	-17.4
5	12	3	29.9	-32.9	-1	14	6	38.3	-44.2	-2	13	4	17.1	8.3	-3	10	3	19.7	-19.8	-4	8	3	46.1	-47.6
5	13	3	25.1	-27.6	-1	15	6	19.5	-21.2	-2	14	4	27.5	20.6	-3	11	3	36.1	-33.8	-4	9	3	24.2	-29.4
5	14	3	30.7	-32.1	-1	16	6	15.8	19.6	-2	16	4	43.3	-41.8	-3	12	3	28.0	32.9	-4	10	3	29.8	-26.7
5	1	4	16.3	-15.8	-1	17	6	20.4	-20.7	-2	17	4	16.5	-16.3	-3	13	3	61.5	-61.8	-4	11	3	22.9	20.5
5	2	4	18.1	19.0	-1	18	6	73.0	77.3	-2	18	4	13.8	-15.5	-3	14	3	57.9	-61.0	-4	12	3	16.9	-12.1
5	3	4	15.4	-12.0	-1	19	6	23.7	26.8	-2	19	4	36.7	34.0	-3	15	3	31.6	31.6	-4	13	3	33.8	-34.6
5	4	4	22.4	-26.5	-1	20	6	39.3	39.3	-2	20	4	43.0	-42.7	-3	16	3	38.6	-37.6	-4	14	3	95.4	51.2
5	5	4	11.4	10.7	-1	2	7	73.2	75.8	-2	0	5	39.6	50.4	-3	17	3	57.9	63.2	-4	2	4	11.4	-28.4
5	5	4	20.2	-21.9	-1	4	7	27.1	-27.9	-2	2	5	21.4	-17.7	-3	18	3	74.5	-24.3	-4	3	4	61.6	61.6
5	7	4	14.4	-16.7	-1	5	7	36.1	-35.4	-2	3	5	119.7	121.2	-3	20	3	17.7	-17.7	-4	4	4	30.2	31.5
5	7	4	305.6	351.4	-1	6	7	35.8	-35.6	-2	4	5	34.1	-34.1	-3	21	3	87.3	84.7	-4	5	4	16.8	-16.8
5	8	4	56.0	53.3	-1	9	7	30.8	20.7	-2	5	5	50.1	-46.2	-3	2	4	26.9	29.4	-4	6	4	58.0	-58.4
5	10	4	238.6	250.9	-1	12	7	30.9	-29.9	-2	6	5	77.1	-78.0	-3	3	4	25.2	-26.4	-4	7	4	71.4	-74.4
5	12	4	47.5	-44.1	-1	13	7	23.2	20.5	-2	7	5	192.9	-106.2	-3	4	4	35.8	-29.9	-4	8	4	16.8	-11.4
5	14	4	135.7	-135.9	-1	14	7	36.7	-34.4	-2	8	5	34.7	-34.4	-3	5	4	93.3	99.3	-4	9	4	20.8	18.6
5	16	4	33.5	37.4	-1	15	7	15.6	-14.7	-2	9	5	58.9	57.6	-3	6	4	67.6	68.4	-4	10	4	61.4	59.7
5	18	4	109.6	-109.4	-1	17	7	36.0	36.6	-2	10	5	46.4	45.1	-3	7	4	34.5	32.6	-4	11	4	17.9	-16.4
5	1	4	80.4	83.1	-1	18	7	24.4	-23.7	-2	11	5	55.0	57.7	-3	8	4	42.7	-46.1	-4	12	4	28.6	-28.6
5	1	4	92.9	-92.5	-1	0	8	33.0	33.3	-2	12	5	36.7	34.0	-3	9	4	36.4	33.6	-4	13	4	16.7	-16.7
5	10	4	76.6	80.0	-1	1	8	13.9	-14.9	-2	13	5	96.2	-80.2	-3	10	4	36.0	30.9	-4	14	4	14.9	26.7
5	11	4	62.9	-58.7	-1	2	8	18.0	17.8	-2	16	5	41.9	39.9	-3	17	4	12.0	-10.7	-4	15	4	29.6	-36.3
5	13	4	49.6	51.4	-1	3	8	20.1	19.9	-2	17	5	32.9	33.1	-3	18	4	35.9	-32.5	-4	16	4	15.5	-15.1
5	14	4	78.8	83.8	-1	4	8	20.5	-14.8	-2	18	5	63.2	66.0	-3	19	4	75.5	-76.9	-4	17	4	15.4	12.6
5	1	4	22.0	23.7	-1	5	8	116.2	113.9	-2	19	5	20.5	-22.2	-3	20	4	47.8	-50.6	-4	18	4	68.2	-68.2
5	19	4	22.6	-21.9	-1	7	8	23.0	-19.3	-2	0	6	32.4	-36.9	-3	2	5	23.3	20.0	-4	7	5	26.2	31.1
5	20	4	34.7	-37.5	-1	8	8	23.4	23.4	-2	1	6	40.5	40.6	-3	3	5	36.3	-37.8	-4	8	5	29.6	-25.7
5	21	4	35.5	37.2	-1	9	8	17.1	-15.1	-2	2	6	52.4	-53.0	-3	4	5	72.7	-74.4	-4	9	5	40.7	39.4
5	22	4	31.1	17.9	-1	10	8	34.8	-34.5	-2	3	6	22.8	16.9	-3	5	5	36.6	32.2	-4	10	5	16.6	-16.6
5	1	4	35.4	-34.4	-1	11	8	19.6	20.0	-2	4	6	40.2	-34.2	-3	6	5	19.4	-29.5	-4	11	5	14.9	26.7
5	11	4	62.9	-58.7	-1	2	8	18.0	17.8	-2	16	5	41.9	39.9	-3	17	4	12.0	-10.7	-4	12	5	29.6	-36.3
5	13	4	49.6	51.4	-1	3	8	20.1	19.9	-2	17	5	32.9	33.1	-3	18	4	35.9	-32.5					

might indicate that the carbon-carbon and iron-carbon distances of the π -bonded cyclopentadienyl ring are not all equivalent. All of these features will be discussed later in some detail.

The structure of CIMH unambiguously contains no bridging carbonyls. Although recently Dahm and Jacobson¹ noted the existence of asymmetric bridging carbonyls in $\text{Fe}_3(\text{CO})_{11}\text{P}(\text{C}_6\text{H}_5)_3$ any assumption that one or more of the carbonyls in CIMH forms an asymmetric bridge across the Fe-Mn bond would necessitate the existence of a metal-carbon bond of at least 2.99 Å in length, this being the shortest metal to carbonyl carbon "nonbonded" distance (as shown in Table 4). Such a bond would certainly be out of the question. The longest corresponding distance in $\text{Fe}_3(\text{CO})_{11}\text{P}(\text{C}_6\text{H}_5)_3$ is only 2.08 Å.

The absence of any bridging carbonyls is entirely consistent with the results of infrared studies of the spectra of solutions of CIMH. In general, terminal carbonyl stretching frequencies occur in the range of 1850-2100 cm^{-1} , while bridging carbonyl stretching frequencies lie in the range of 1750-1875 cm^{-1} . Although exceptions to these generalizations have been pointed out by Cotton and Wilkinson (21), these exceptions should not apply in the case of CIMH. King, Treichel and Stone (6) noted the following absorption bands in the infrared spectrum of a C_2Cl_4 solution of CIMH: 2078, 2052, 2012, 1982 and 1941 cm^{-1} . Furthermore a spectrum obtained in this laboratory using a CCl_4 solution showed seven absorption bands at the following positions: 2078, 2050, 2011, 1996, 1988, 1974 and

¹Dahm, D. J. and Jacobson, R. A. Department of Chemistry, Iowa State University of Science and Technology, Ames, Iowa. Crystal structure of $\text{Fe}_3(\text{CO})_{11}\text{P}(\text{C}_6\text{H}_5)_3$. Private communication. 1966.

1939 cm^{-1} . But, in both cases the absorption band of lowest frequency lies considerably above what is normally considered as the upper limit of the bridging carbonyl stretching region, i.e. 1875 cm^{-1} .

Regarding the metal-metal linkage, the structure is thus quite similar to the $\text{Mn}_2(\text{CO})_{10}$ structure and quite unlike the $[\pi\text{-C}_5\text{H}_5\text{Fe}(\text{CO})_2]_2$ structure in that the two moieties are held together solely by an Fe-Mn bond of length 2.843 Å.

It is noteworthy that the two crystallographically independent molecules in the CIMH structure do not assume identical conformations. This can clearly be seen in Figure 3, where each molecule has been projected onto a plane which is perpendicular to its iron-manganese bond. The difference in the amount of the internal rotation about the metal-metal bond appears to be approximately seven degrees. Also from Figure 3 it can be seen that any conformation which staggers the iron carbonyls precisely between the equatorial manganese carbonyls results in the eclipsing of atom C_8 and the hydrogen atom bonded to it (H_8), and conversely any conformation which staggers atoms C_8 and H_8 precisely between the equatorial manganese carbonyls results in the almost perfect eclipsing of the iron carbonyls. Thus if one were to construct a plot of potential energy versus the angle of internal rotation, one would expect the energy minima to be quite broad. In addition, since the two molecules are crystallographically independent, the environment surrounding, and consequently the intermolecular forces affecting each molecule must (by definition) be different. In light of these two conditions it is indeed not surprising that the conformational difference exists.

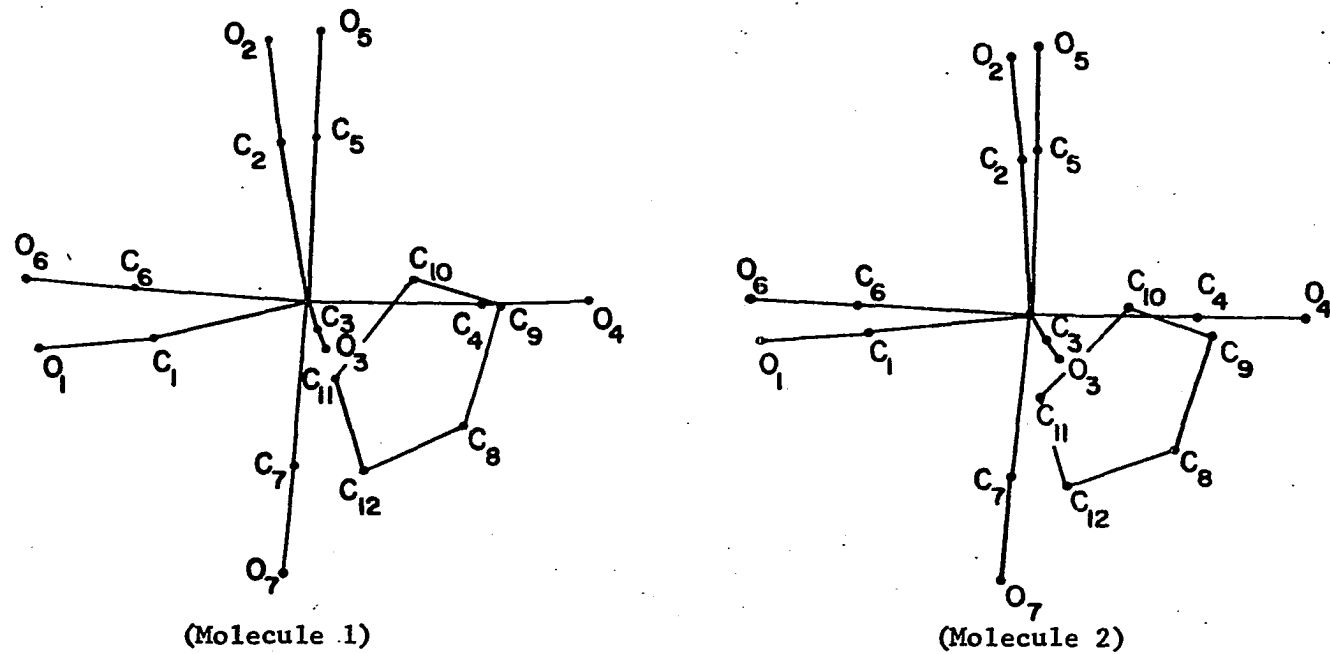


Figure 3. The conformations of the two crystallographically independent molecules

Manganese Moiety

A close look at the geometry of the $\text{Mn}(\text{CO})_5$ portion of the CIMH molecule, and in particular a comparison of this group with the same or similar group found in other previously determined structures has proven to be most interesting. An examination of the manganese-carbon and carbon-oxygen average bond distances listed in Table 3 reveals a distinct difference between the axial and equatorial carbonyls of the $\text{Mn}(\text{CO})_5$ moiety. For the equatorial carbonyls the average Mn-C distance is 1.825 \AA and the average C-O distance is 1.156 \AA while for the axial carbonyls the average Mn-C distance is 1.749 \AA and the average C-O distance is 1.195 \AA . Thus the axial Mn-C and C-O bond lengths appear to be respectively 0.076 \AA shorter and 0.039 \AA longer than their equatorial counterparts.

Table 6 contains a list of these distances and differences together with the corresponding values found in several related structures. It may be seen that the axial and equatorial Mn-C distances differ only slightly and the corresponding C-O distances only negligibly in both the $\text{Mn}_2(\text{CO})_{10}$ structure and the $\text{HMn}(\text{CO})_5$ structure. In fact LaPlaca, Hamilton and Ibers (22) in their paper on the crystal and molecular structure of $\text{HMn}(\text{CO})_5$ explicitly state that "the shortening of the apical Mn-C bond, if real, is surely small." In light of these comparisons alone, the results of this structure determination might be viewed with some skepticism; however, recently Bailey and Dahl (23) reported an even greater disparity between these axial and equatorial distances in the technetium analog to $\text{Mn}_2(\text{CO})_{10}$, i.e. $\text{Tc}_2(\text{CO})_{10}$. As may be seen in Table 6, the axial Tc-C and C-O bond lengths are respectively 0.101 \AA shorter and 0.084 \AA longer

Table 6. Comparison of equivalent mean angles, distances and differences found in CIMH and related structures together with their estimated standard errors (distances and differences in Å and angles in degrees)

Atoms ^a	CIMH	HMn(CO) ₅ ^b	Mn ₂ (CO) ₁₀ ^c	Tc ₂ (CO) ₁₀ ^d
M-C _{equatorial}	1.825(9)	1.840(4)	1.831(8)	2.000(6)
M-C _{axial}	1.749(18)	1.821(9)	1.792(14)	1.899(11)
Δ (M-C)	0.076(20)	0.019(10)	0.038(16)	0.101(12)
C-O, equatorial	1.156(8)	1.130(5)	1.157(8)	1.121(6)
C-O, axial	1.195(17)	1.131(9)	1.151(16)	1.205(13)
Δ (C-O)	-.039(19)	-.001(10)	0.006(18)	-.084(14)
C _{eq} -M-C _{ax}	93.4(4)	96.7(2)	93.8(3)	93.8(2)
M'-M-C _{ax}	168.9(6)	_e	177.3(5)	177.3(4)

^aM refers to the metal to which the carbonyls are bonded and M' to the second metal.

^bSource: (22).

^cSource: (9).

^dSource: (23).

^eThe position of the hydrogen atom was not observed.

than their equatorial counterparts.

Before accepting such a disparity, however, the infrared spectrum should be consulted. Examination of the infrared spectrum, previously mentioned and tabulated in Table 7, reveals the existence of no peaks with a frequency lower than 1939 cm^{-1} . Since a carbonyl bond length of 1.195 Å approaches that expected for a bridging carbonyl, one might expect that

the infrared spectrum of CIMH would show an absorption band in or near the bridging carbonyl stretching frequency range of approximately 1750-1875 cm^{-1} . In fact, Margoshes et al. (24) fitted a smooth curve to a plot of bond length versus stretching frequency of the carbonyl group for a series of eighteen compounds with C-O bond lengths ranging from 1.13 to 1.31 Å and found the average deviation from the line to be only 0.013 Å. According to this curve, a C-O bond length of 1.195 Å (the axial C-O bond length in CIMH) corresponds to a stretching frequency of slightly less than 1800 cm^{-1} . However, one should bear in mind two factors: first of all the theoretical basis for the simple relationship observed by Margoshes et al. includes a simplifying assumption involving the motion of the atoms and the relationship is thus not expected to hold in all cases (in fact, one point of their plot deviated from the smooth curve by 0.0525 Å) and secondly, the infrared spectrum of CIMH was obtained using a CCl_4 solution rather than a solid sample, and this could conceivably be responsible for some shift in absorption frequency. Furthermore, an excellent counter-example is provided by a comparison of both the infrared spectra and C-O bond distances of $\text{Mn}_2(\text{CO})_{10}$ and $\text{Tc}_2(\text{CO})_{10}$. As may be seen in Table 6, the equatorial C-O distances of these two compounds differ by 0.036 Å and the axial C-O distances differ by 0.054 Å; yet, as shown in Table 7, the infrared spectra of the carbonyl stretching region of these compounds are almost identical. Thus it certainly would not be correct to conclude that the results of this structure determination are incompatible with the results of infrared studies.

It is very unlikely that the long C-O distance and the short Mn-C distance found for the axial carbonyl are merely the result of random

Table 7. Infrared absorption bands in the carbonyl stretching region for CIMH and related compounds (in cm^{-1})

CIMH	$\text{Mn}_2(\text{CO})_{10}^a$	$\text{Ta}_2(\text{CO})_{10}^a$
1939 (w)	1949 (vw)	1950 (vw)
1974 (sh)	1956 (vw)	1964 (vw)
1988 (vs)	1983 (m)	1984 (m)
1996 (sh)	1993 (vw)	1997 (vw)
2011 (m)	2001 (w)	2006 (w)
2050 (s)	2013 (vs)	2017 (vs)
2078 (s)	2044 (m)	2065 (m)

^aSource: (25).

errors in the axial carbon positional parameters, since there are two crystallographically independent molecules in this structure and as may be seen in Table 3, the agreement between the two molecules for these distances is excellent.

Although conceivably a systematic error might have been responsible for these results, no good reason for expecting this to be the case has ever been uncovered. Dahl and Rundle (9) noted that an anisotropic refinement resulted in a rather large shift of the axial carbon atom in $\text{Mn}_2(\text{CO})_{10}$ from the position found by an isotropic refinement; however, most likely the anisotropy of the manganese atom rather than that of the carbon atom was responsible for this shift. And, although the light atoms in the CIMH structure were refined only isotropically, the heavy atoms did receive an anisotropic refinement.

All in all, from an empirical standpoint, there appears to be little if any reason to doubt the reality of--or in fact the magnitude of--the observed bond length difference between the axial and equatorial carbonyls. And furthermore, from a theoretical standpoint these differences can also be quite reasonably explained qualitatively. However, before discussing this theoretical basis, a very brief discussion of the metal-carbonyl bonding mechanism, as it is presently understood, will be presented. More thorough discussions may be found elsewhere in any of several standard texts (21,26,27,28).

Transition metal-carbonyl bonds owe their remarkable stability to the formation of a multiple bond having both σ and π character. The σ bonding may be thought of as resulting from the rather strong overlap of the CO lone pair of electrons of the carbon σ orbital with an empty σ orbital of the metal atom. (In the case of an octahedral first row transition metal complex the latter might be a $3d_{\sigma}$, $4s$ or $4p$ AO or in valence bond language a d^2sp^3 hybrid.) This σ bond would result in the transfer of appreciable electron density to the metal atom. On the other hand the π bonding may be thought of as resulting from the overlap of filled or partially filled d_{π} orbitals of the metal atom with rather low lying (due to unsaturation) π^* antibonding MO's of the carbonyl. (For an octahedral first row transition metal, these would be the $3d$ orbitals, i.e. $3d_{xy}$, $3d_{xz}$ and $3d_{yz}$.) This is often referred to as back donation. It may be noted that this π bonding results in the transfer of electron density from the metal to the carbonyl, i.e. in the direction opposite to that resulting from the σ bonding. This bonding mechanism (including both the σ and π bonding) has been referred to by some as "synergic" in

that the two modes of bonding tend to strengthen or complement each other.

Now, from an extension of this bonding mechanism to the case of the $\text{Mn}(\text{CO})_5$ moiety the axial-equatorial bond differences can be quite simply explained. Consider a Cartesian coordinate system with the manganese atom at the origin, the axial carbonyl lying along the z axis and the four equatorial carbonyls lying approximately along the x and y axes. (The equatorial carbonyls will not coincide exactly with the x and y axes since, as may be seen in Table 5, the $\text{C}_{\text{eq}}-\text{Mn}-\text{C}_{\text{ax}}$ angles all exceed ninety degrees.) Recalling the preceding paragraph, the π character of the Mn-C bonds in the $\text{Mn}(\text{CO})_5$ moiety results from the overlap of the filled $3d_{xy}$, $3d_{yz}$ and $3d_{xz}$ orbitals of the manganese atom with π^* MO's from the carbonyls. More specifically, the two equatorial carbonyls lying along the x axis employ the $3d_{xy}$ and $3d_{xz}$ orbitals, the two equatorial carbonyls lying along the y axis employ the $3d_{xy}$ and $3d_{yz}$ orbitals and the lone axial carbonyl employs the $3d_{yz}$ and $3d_{xz}$ orbitals. It can thus be seen that the $3d_{xy}$ orbital is employed by four carbonyls while both the $3d_{xz}$ and $3d_{yz}$ orbitals are employed by only three. The shortening of the axial Mn-C bond can thus be attributed to what might be called a "trans effect" since trans to each equatorial carbonyl lies another equatorial carbonyl with which it must "compete" for the electrons of two 3d orbitals, while the axial carbonyl lies trans to the iron atom whose bond to the manganese atom does not use any of the 3d orbitals and thus poses no such "competitive threat". In fact the strength of the iron-manganese bond would most likely be enhanced by increased back donation to the carbonyls by the $3d_{xz}$ and $3d_{yz}$ orbitals since these same two 3d orbitals on the iron atom are also filled. (This may explain the

observation that the Mn-C bond distances in CIMH and in $\text{Mn}_2(\text{CO})_{10}$ are shorter than the corresponding Mn-C bond distances in $\text{HMn}(\text{CO})_5$; although in light of the size of the standard errors involved these differences must be viewed with a certain amount of skepticism.)

Furthermore, the inverse relationship which has been frequently observed between a change in length of a metal-CO bond and a change in length of the corresponding C-O bond may also be explained on a theoretical basis. As a C-O bond is lengthened, its π bond becomes weaker and subsequently the π^* antibonding orbitals drop in energy and more nearly match the energy of the 3d orbitals of the metal atom. This results in an increase in the π bonding between the metal and the carbonyl and consequently a shorter metal-carbon bond. Conversely, by similar reasoning, if a metal-carbon bond is shortened (as with the axial Mn-C bond of the $\text{Mn}(\text{CO})_5$ moiety) the corresponding C-O bond should lengthen (29,30).

A comparison of the bond angles in the $\text{Mn}(\text{CO})_5$ moiety contained in CIMH with those found in $\text{HMn}(\text{CO})_5$, $\text{Mn}_2(\text{CO})_{10}$ or $\text{Tc}_2(\text{CO})_{10}$ reveals similarities, but also some rather striking differences. In all four structures the equatorial carbonyls are bent away from the axial carbonyl such that the $\text{C}_{\text{eq}}-\text{Mn}-\text{C}_{\text{ax}}$ angles exceed ninety degrees. The average values for these angles are listed in Table 6. Quite probably axial-equatorial C...C repulsions are responsible for this effect and in addition the larger angles found in $\text{HMn}(\text{CO})_5$ are probably due to the presence of a much less bulky group trans to the axial carbonyl.

In CIMH, the values of the $\text{Fe}-\text{Mn}-\text{C}_{\text{ax}}$ angle were found to be 168.6° and 169.2° for the two independent molecules. These values differ from 180° by approximately fourteen times the estimated standard deviations

and are thus undoubtedly statistically significant. This nonlinearity represents a substantial distortion from the expected octahedral coordination and probably results from the repulsive forces acting between the two iron carbonyls and the two manganese carbonyls in closest proximity (see Figures 1 and 3). Interestingly, the metal-metal-axial carbon angles in $\text{Mn}_2(\text{CO})_{10}$ and in $\text{Tc}_2(\text{CO})_{10}$ were found to be $177.3 \pm 0.5^\circ$ and $177.3 \pm 0.4^\circ$ respectively. Although on the surface these may appear to be very close to 180° , the actual difference (2.7°) represents respectively five and seven times the reported standard deviations. If one assumes that the reported standard deviations are correct, it is quite improbable that the true value of this angle could be as large as 180° in either of these two molecules, although no mention of this apparent abnormality is found in the literature (9,23).

Since the equatorial carbonyls in the $\text{Mn}(\text{CO})_5$ moiety are all bent away from the axial carbonyl, one might expect the angles defined by two adjacent equatorial carbon atoms and a manganese atom (at the vertex) i.e. $\text{C}_{\text{eq}}-\text{Mn}-\text{C}_{\text{eq}}$, to be acute; however, in CIMH one of these angles in each molecule, the $\text{C}_7-\text{Mn}-\text{C}_4$ angle is notably larger than ninety degrees. The two values of this angle are 92.3° and 93.7° versus an average of 88.7° for the other six members of the set. This effect is apparently due to the close proximity of the cyclopentadienyl ring and in particular atom C_8 and the hydrogen atom affixed to it (see Figures 1 and 3). It may be seen in Table 5 that angles $\text{Fe}-\text{Mn}-\text{C}_4$ and $\text{Fe}-\text{Mn}-\text{C}_7$ are significantly smaller than angles $\text{Fe}-\text{Mn}-\text{C}_5$ and $\text{Fe}-\text{Mn}-\text{C}_6$, indicating that the Fe-Mn bond is "bent" towards the opening between carbonyls four and seven. In the $\text{HMn}(\text{CO})_5$ structure all of the aforementioned $\text{C}_{\text{eq}}-\text{Mn}-\text{C}_{\text{eq}}$ angles are acute, as one

would expect in view of the nearly perfect fourfold symmetry of the molecule. In the $\text{Mn}_2(\text{CO})_{10}$ structure the largest of these four angles equals 91.6° and the average of the other three angles equals 89.2° (reported individual standard deviations 0.6°). The corresponding values for the $\text{Tc}_2(\text{CO})_{10}$ structure are 90.4° and 89.6° (reported individual standard deviations 0.4°). Although the statistical significance of these variations is certainly questionable, it is noteworthy that these two crystal structures are isomorphous and that the two "large" angles are homologous.

Iron Moiety

The iron moiety in CIMH will be discussed as two separate systems; the first includes the iron atom and the two terminal carbonyl groups bonded to it, while the second includes the iron atom and the π -bonded cyclopentadienyl ring. Although the Mn-C-O angles in CIMH all appear to be within experimental error of 180° (the maximum deviation being 2.9° and the individual standard deviations averaging about 2.0°), the Fe-C-O angles range from 169.5° to 173.9° (the individual standard deviations again averaging about 2.0°) and are therefore most assuredly nonlinear. Although at first glance this may appear to be rather surprising, S. F. A. Kettle in a recent article (31) stated "that bending of the M-C-O chain is to be expected" in $\text{M}(\text{CO})_2$, $\text{M}(\text{CO})_3$ and $\text{M}(\text{CO})_4$ groups. (Where M represents a transition metal atom.) The article provided some rather convincing arguments in support of this belief, together with references to eight structures in which this phenomenon has been observed. His argument is based on the fact that with groups of this type there is no

symmetry requirement that the two sets of π^* orbitals of the carbonyls must interact equally with the metal orbitals and it thus follows that a linear M-C-O fragment is not required.

Table 8 contains the Fe-C distances and the corresponding C-O distances reported for several compounds whose structures have been determined in recent years. Although the statistical significance may in some cases be doubtful, the average Fe-C distance reported for each of the four structures is longer than the value of 1.716 Å found in CIMH, and with the exception of the $\text{Fe}(\text{CO})_3(\text{C}_6\text{H}_5\text{C}_2\text{C}_6\text{H}_5)_2$ structure the average C-O bond lengths are somewhat shorter than the value of 1.169 Å found in CIMH. This appears to be another example of the inverse relationship between metal-carbon and carbon-oxygen bond lengths found in transition metal carbonyls, as discussed previously.

Table 8. Mean iron carbonyl distances and standard errors in related structures (in Å).

Structure	Fe-C	C-O
$\text{Fe}(\text{CO})_3(\text{C}_6\text{H}_5\text{C}_2\text{C}_6\text{H}_5)_2^a$	1.750(13)	1.179(17)
$\text{Fe}(\text{CO})_5^b$	1.78(3)	1.12(3)
$\text{C}_4\text{H}_6\text{Fe}(\text{CO})_3^c$	1.76(4)	1.15(5)
$[\text{SFe}(\text{CO})_3]_2^d$	1.776(12)	1.142(15)

^aSource: (32).

^bSource: (33).

^cSource: (34).

^dSource: (35).

Since the discovery of ferrocene in 1951 (36,37) an enormous amount of research has been carried out on compounds containing a cyclopentadienyl ring π -bonded to a transition metal atom. No attempt shall be made here to summarize either the chemistry of these compounds nor the various bonding theories which have been proposed. Both of these topics are quite thoroughly covered in an excellent review article by Cotton and Wilkinson (38). (The list of references alone in this article consumes fourteen pages!) The present discussion of the π -cyclopentadienyl iron system in the CIMH structure shall be limited to some rather unexpected findings concerning the equivalency of the C-C and Fe-C_{ring} distances, together with a comparison of these distances with those found in related structures.

Early in the analysis of the results of this crystal structure determination, a marked ordering of the deviations of the individual C-C and Fe-C_{ring} distances from their respective mean values was noted. As may be seen in Table 3, in both molecules the C₈-C₉ distance is the longest, the C₉-C₁₀ and C₁₁-C₁₂ distances are respectively the second and third longest, and the C₁₀-C₁₁ and C₁₂-C₈ distances are the shortest. Likewise a similar pattern exists within the set of ten Fe-C_{ring} distances. It is quite improbable that ordering of such a high degree as this would occur if these distances were indeed truly equivalent. There thus appears to be some basis for believing that these distances are not all equivalent. (It should be noted that neither ring deviates significantly from perfect planarity. The maximum deviation of a carbon atom from the least squares plane is 0.011 Å and the average deviation is only 0.006 Å.)

Since there have been reports of other structures of this type in which these distances were not equivalent the existence of non-equivalent

C-C and Fe-C_{ring} distances in this structure should not have been surprising. Theoretical explanations which might account for these bonds being chemically non-equivalent have been given by Dahl and Wei (39), employing a simple valence bond approach, and by Burnett *et al.* (40), using a molecular orbital treatment.

Nevertheless, it is felt that the magnitudes of the differences detected in this structure are not large enough for firm conclusions to be drawn. And it is conceivable that these results might merely be due to steric or packing effects, or to some systematic error.

The average C-C distance of 1.403 Å and the average Fe-C_{ring} distance of 2.104 Å found for the CIMH structure compare very favorably with those found in ferrocene itself and with those found in $[\pi\text{-C}_5\text{H}_5\text{Fe}(\text{CO})_2]_2$. The corresponding distances found in ferrocene by Dunitz, Orgel and Rich (41) using a least squares analysis were respectively 1.409 Å and 2.048 Å (individual standard deviations 0.035 Å and 0.031 Å). Average values of 1.41 Å and 2.11 Å were found for these distances by Mills (8) in the $[\pi\text{-C}_5\text{H}_5\text{Fe}(\text{CO})_2]_2$ structure (standard deviations 0.04 Å and 0.03 Å respectively).

In several cases the results of this crystal structure determination have suggested to the author problems for further study and investigation. Three of these are included in the research propositions given in Appendix B.

LITERATURE CITED

1. Mond, L., Langer, C. and Quincke, F. J. Chem. Soc. 57: 749. 1890.
2. Mond, L. and Quincke, F. J. Chem. Soc. 59: 604. 1891.
3. Abel, E. W., Singh, A. and Wilkinson, G. J. Chem. Soc. 1321. 1960.
4. Chini, P., Colli, L. and Peraldo, M. Gazz. Chim. Ital. 90: 1005. 1960.
5. Tilney-Basset, J. F. Proc. Chem. Soc. 419. 1960.
6. King, R. B., Treichel, P. M. and Stone, F. G. A. Chem. Ind. (London) 747. 1961.
7. Joshi, K. K. and Pauson, P. L. Z. Naturforsch. 17b: 565. 1962.
8. Mills, O. S. Acta Cryst. 11: 620. 1958.
9. Dahl, L. F. and Rundle, R. E. Acta Cryst. 16: 419. 1963.
10. International tables for X-ray crystallography. Vol. 1. Birmingham, England, Kynoch Press. 1959.
11. Lawton, S. L. and Jacobson, R. A. U.S. Atomic Energy Commission Report IS-1141 [Iowa State University of Science and Technology, Ames. Institute for Atomic Research]. 1965.
12. Williams, D. E. U.S. Atomic Energy Commission Report IS-1052 [Iowa State University of Science and Technology, Ames. Institute for Atomic Research]. 1964.
13. Wehe, D. J., Busing, W. R. and Levy, H. A. U.S. Atomic Energy Commission Report ORNL-TM-299 [Oak Ridge National Laboratory, Oak Ridge, Tennessee]. 1962.
14. International tables for X-ray crystallography. Vol. 3. Birmingham, England, Kynoch Press. 1962.
15. Williams, D. E. and Rundle, R. E. J. Am. Chem. Soc. 86: 1660. 1964.
16. Vand, V. and Dunning, A. J. Am. Cryst. Assoc., Gatlinburg, Tenn., June 27-July 2, 1965, Program and Abstracts 1965: 78. 1965.
17. Jacobson, R. A., Wunderlich, J. A. and Lipscomb, W. N. Acta Cryst. 14: 598. 1961.
18. Hanson, H. P., Herman, F., Lea, J. D. and Skillman, S. Acta Cryst. 17: 1040. 1964.

19. Busing, W. R., Martin, K. O. and Levy, H. A. U.S. Atomic Energy Commission Report ORNL-TM-306 [Oak Ridge National Laboratory, Oak Ridge, Tennessee]. 1964.
20. Hamilton, W. C. *Acta Cryst.* 12: 609. 1959.
21. Cotton, F. A. and Wilkinson, G. *Advanced inorganic chemistry*. New York, N.Y., Interscience Publishers. 1962.
22. LaPlaca, Sam J., Hamilton, Walter C. and Ibers, James A. *Inorg. Chem.* 3: 1491. 1964.
23. Bailey, Marcia F. and Dahl, Lawrence F. *Inorg. Chem.* 4: 1140. 1965.
24. Margoshes, M., Fillwalk, F., Fassel, V. A. and Rundle, R. E. *J. Chem. Phys.* 22: 381. 1954.
25. Flitcroft, N., Huggins, D. K. and Kaesz, H. D. *Inorg. Chem.* 3: 1123. 1964.
26. Richardson, James W. *Am. Chem. Soc. Monograph No.* 147: 1. 1960.
27. Pauling, Linus. *The nature of the chemical bond*. 3rd ed. Ithaca, N.Y., Cornell University Press. 1960.
28. Orgel, L. E. *An introduction to transition-metal chemistry: ligand-field theory*. New York, N.Y., John Wiley and Sons, Inc. 1963.
29. Cotton, F. A. and Kraihanzel, C. S. *J. Am. Chem. Soc.* 84: 4432. 1962.
30. Cotton, F. A. and Wing, R. M. *Inorg. Chem.* 4: 1328. 1965.
31. Kettle, S. F. A. *Inorg. Chem.* 4: 1661. 1965.
32. Dodge, R. P. and Schomaker, V. *Acta Cryst.* 18: 614. 1965.
33. Donohue, Jerry and Caron, Aimery. *Acta Cryst.* 17: 663. 1964.
34. Mills, O. S. and Robinson, G. *Acta Cryst.* 16: 758. 1963.
35. Wei, Chin Hsuan and Dahl, Lawrence F. *Inorg. Chem.* 4: 1. 1965.
36. Kealy, T. J. and Pauson, P. L. *Nature* 168: 1039. 1951.
37. Miller, S. A., Tebboth, J. A. and Tremaine, J. F. *J. Chem. Soc.* 632. 1952.
38. Cotton, F. A. and Wilkinson, G. *Progr. Inorg. Chem.* 1: 1. 1959.
39. Dahl, L. F. and Wei, C. H. *Inorg. Chem.* 2: 713. 1963.

40. Burnett, M. J., Churchill, M. R., Gerloch, M. and Mason, R. *Nature* 201: 1318. 1964.
41. Dunitz, J. D., Orgel, L. E. and Rich, Alexander. *Acta Cryst.* 9: 373. 1956.
42. Housty, Par J. and Hospital, M. *Acta Cryst.* 18: 693. 1965.
43. Coppens, Philip and Schmidt, G. M. J. *Acta Cryst.* 18: 654. 1965.
44. Katz, Lewis and Lipscomb, William N. *Acta Cryst.* 5: 313. 1952.
45. Scarborough, J. B. *Numerical mathematical analysis*. 4th ed. Baltimore, Md., John Hopkins Press. 1958.
46. Popov, A. I., Geske, D. H. and Baenziger, N. C. *J. Am. Chem. Soc.* 78: 1793. 1956.

APPENDIX A

Direct Methods Research

Whereas the determination of the crystal structure of CIMH involved, for the most part, the application of well known and understood crystallographic methods to a compound whose crystal structure was totally unknown; a substantial amount of time and effort was also expended on a problem which involved the application of some totally new and untried crystallographic methods to several previously solved crystal structures and to some simple hypothetical structures. Prior to beginning this latter problem, it was well understood that the probability of attaining what could be properly called success was probably very small, but yet it was thought that the significance of this success if attained would be sufficiently great as to warrant the undertaking of the problem.

Although basically only two different methods were examined, each of these underwent numerous modifications and changes. Both methods were what are generally referred to as "direct methods"; that is they attacked the problem of determining the phases in a purely mathematical fashion, as opposed for example, to such methods as the Patterson superposition or the "heavy atom" technique.

Although the results of this work were, for the most part, quite unfavorable it is felt that "for the record" some report of this work should be made. Since both methods have at times shown some promise, it is also conceivable that one of them might be used in conjunction with some other method(s), either direct or indirect, or that some other more imaginative or ingenious worker might be able to develop one of these

methods into a more usable and practical form; in either case this account could provide a foundation for further work.

Both methods were applicable to centrosymmetric structures only (in which the phase problem is reduced to that of determining the correct signs of the observed structure factors).

The first of these two methods is based on the following assumptions:

1. The electron density at any point in a crystal may be zero or positive, but never negative.
2. The electron density function can be rather accurately represented by a Fourier series expansion using only a relatively small number of the structure factors (i.e. Fourier coefficients) such that assumption one will still in general be true.
3. It can be shown that the integral of the electron density function, $\rho(\vec{r})$, over the entire volume of the unit cell is equal to $F(000)$, i.e. the number of electrons in the unit cell. Furthermore, in view of assumptions one and two, if the integrand, $\rho(\vec{r})$, is replaced by its absolute value, $|\rho(\vec{r})|$, the result of this integration remains the same. However, if one considers the pseudo electron density function, $\rho'(\vec{r})$ (which is the Fourier series expansion of $\rho(\vec{r})$ in which the signs of the structure factors may not all be correct), these results are somewhat altered. The integral of $\rho'(\vec{r})$ over the volume of the unit cell is again equal to $F(000)$, since the value of this integral is invariant to the signs of the structure factors (except $F(000)$, which is known to be positive), but if one replaces $\rho'(\vec{r})$ by its absolute value, $|\rho'(\vec{r})|$, the result will in general be greater than $F(000)$ since the pseudo electron density function is not restricted to positive or zero values, and presumably will equal

$F(000)$ only when the signs are all correct (in which case $\rho'(\vec{r})$ and $\rho(\vec{r})$ are identical). Furthermore, it is assumed that the greater the value of this integral the more incorrect is the particular set of structure factor signs being considered and that to a good approximation the value of this integral can be obtained by performing a summation, providing one chooses a sufficiently small grid. Thus basically this method consists in the minimization of $\sum |\rho'(\vec{r})|$ with respect to the signs of the structure factors included in the Fourier series expansion of the electron density function.

4. It was assumed that this minimization could be accomplished using a type of steepest descents method. Beginning with an initial set of structure factor signs (which would be entirely random in the case of an undetermined structure) a pseudo electron density map was calculated and its absolute value summed as previously mentioned. Sequentially, the sign of one and only one structure factor was changed from that of the initial set and the previous step was repeated until the sign of every structure factor had been reversed for one calculation and summation. (Thus if there were N structure factors, $N + 1$ calculations and summations would have been performed and in each case $N - 1$ structure factors would have the same sign as possessed in the initial set.) The values of the sums were then compared, and for the next cycle the initial set of structure factor signs would be identical to those of this cycle except that the structure factor whose sign reversal resulted in the smallest sum would have the opposite sign. This whole process was then repeated over and over until the value of the sum would no longer decrease.

The vast majority of the time and effort expended on this problem

was devoted to the writing and debugging of computer programs. Initially the main program which was written incorporated a three-dimensional Fortran Fourier subprogram which used an electron density map with a $10 \times 10 \times 20$ point grid and was specific to the space group $P2_1/c$. This program was used with data from the adipic acid structure (42); however, even with as few as fifty structure factors the consumption of computer time in testing the method proved to be too large for practical use. Consequently, a two dimensional Fortran Fourier subprogram was written for the plane group pgg with a 20×20 point grid. Using this subprogram the method was applied to the $hk0$ data of the β -modification of *p*-nitrophenol whose space group is $P2_1/a$ (43). Using this two dimensional subprogram with eighty $hk0$ structure factors, one complete cycle (as described in assumption #4) consumed approximately one minute.

In general, when using the eighty largest structure factors with initially random signs, the computations would proceed for approximately twenty cycles and stop, indicating that the sum being minimized would decrease no further. Since the signs were initially random, one would expect approximately half of them (or forty) to be wrong, yet only about twenty signs would ever be changed. Using $hk0$ data, there are actually four different sets of completely correct signs, each corresponding to a different choice of origin, and this made it very difficult to judge whether the method actually resulted in any convergence toward a correct set.

Since the results of the computations beginning with random signs were difficult to evaluate, a procedural change was instituted; rather than beginning with totally random signs, $3/4$ or $7/8$ of the structure

factors were given correct signs, or more precisely signs which corresponded to one of the four correct sets. (Since the structure had previously been solved, these correct signs were readily available.) After doing this, different modifications were made and the effects of the modifications could be more readily evaluated.

The various modifications and changes which were tried included the following:

1. It was noted that the use of the calculated structure factors (rather than the observed structure factors) resulted in an improvement, indicating that the method was somewhat sensitive to errors in the structure factors.

2. Rather than using all of the eighty $hk0$ reflections at once, the structure factors were sorted into groups of even-even, even-odd, odd-even, and odd-odd reflections (where even and odd refer to the Miller indices h and k), and computations were performed using each of these groups separately. However, this approach met with a complete lack of success.

3. Rather than minimizing $\Sigma |\rho'(\vec{r})|$ where $\rho'(\vec{r})$ is the pseudo electron density function, the following sum was minimized:

$$\Sigma [\rho'_-(\vec{r})]^2$$

$$\text{where } \rho'_-(\vec{r}) = \begin{cases} \rho'(\vec{r}) & \text{if } \rho'(\vec{r}) < 0 \\ = 0 & \text{if } \rho'(\vec{r}) \geq 0 \end{cases}$$

It was hoped that this would preferentially eliminate or reduce the most

negative troughs. Although the number of signs corrected was certainly greater than random (i.e. more than 50%) the results were worse than those obtained using the original minimization criterion.

4. It was noted that, in general, the signs of the larger structure factors had a tendency to remain fixed; thus rather than merely changing the sign of the structure factor which produced the largest decrease in the sum being minimized, the product of the decrease in this sum and a weighting factor were examined. The sign which was changed corresponded to the largest decrease in this product. Two different weighting factors were used: one, the square root of the structure factor, and two, the structure factor itself. Although this did result in the changing of the signs of more of the larger structure factors, the overall results were not favorable.

5. In addition to using the ordinary structure factors (both calculated and observed) the method was also used with the unitary structure factors; however, again the results were better than random but yet no more favorable than those obtained using the ordinary structure factors.

These modifications were applied not only singly, but also in various combinations; however, in no case did any substantial improvement result. The most successful trial occurred when using calculated structure factors with $7/8$ of them having the "correct" signs, in which case a completely correct set was obtained after the minimum of ten cycles; however when this factor was changed from $7/8$ to $3/4$, the results were quite unfavorable.

Apparently the "steepest descents" method which was used will result in the program "hanging-up" at a relative minimum when a significant number of signs are wrong. It is recognized that the "steepest descent" method as used here was very crude, but, suitable alternatives could not be found. When one considers that with 80 structure factors there are approximately 2^{80} combinations of signs (which corresponds to an Arabic numeral having about 25 digits) only four of which are correct, one begins to see the complexity of the problem. If, rather than changing one sign at a time, one changes pairs of signs, this alone increases the number of steps per cycle from N to $(N-1)(N-2)/2$ or for the 80 structure factor case, from 80 to 3081.

The second direct method which was investigated has as its basis the following equation:

$$\rho(\vec{r}_0)\rho(\vec{r}_k) = 0$$

where \vec{r}_0 represents a point of zero electron density (commonly referred to as a null point) and where \vec{r}_k corresponds to any other point in the unit cell. Assuming a centrosymmetric structure with n structure factors this equation may be expanded in the following manner:

$$\sum_{i=1}^n \sum_{j=1}^n s_i s_j |F_i| |F_j| \cos(2\pi \vec{h}_i \cdot \vec{r}_0) \cos(2\pi \vec{h}_j \cdot \vec{r}_k)$$

where s_i and s_j represent the appropriate signs of the structure factors F_i and F_j respectively. (Thus s_i and s_j must equal plus or minus one.) Furthermore, if one replaces the various $s_i s_j$ products by x_{ij} 's and notes that $x_{ij} = x_{ji}$ and that $x_{ii} = +1$, this equation may be reduced to the following linear equation:

answers. In the four structure factor case, the ill-conditionedness was eliminated by using more than one null point, but in the nine structure factor case the ill-conditionedness was not eliminated even when every null point of the one dimensional electron density map was used.

In addition to this problem, the null point method in this form possessed a very serious intrinsic limitation owing to the relationship between n , the number of structure factors, and n' , the order of the coefficient matrix to be inverted. Since $n' = n(n-1)/2$, even for as few as 25 structure factors a matrix of order 300 would have to be inverted.

It may be seen that the linear equation given about could be reduced to a nonlinear equation by making the following substitutions for the x_{ij} :

$$x_{ij} = (x_{1i})(x_{1j}),$$

such that the signs of the structure factors are given in terms of their product with the sign of the first structure factor. This reduces the problem from that of solving a set of $n(n-1)/2$ simultaneous linear equations, to that of solving a set of $(n-1)$ simultaneous nonlinear equations. However, it is considerably more difficult to solve simultaneous sets of nonlinear equations, and furthermore, in general more than one solution exists. It was hoped that the latter problem could be overcome by incorporating into the method of solution the further restriction that the roots take on values of plus or minus one only.

Two different techniques for obtaining the desired solution were attempted. The first of these was an extension of the Gauss-Seidel iterative method and the second was the Newton-Raphson method. (No description of either of these methods shall be given here, both are

rather rigorously derived and described elsewhere (45).)

The Gauss-Seidel method necessitates the presence of large diagonal elements and small off-diagonal elements in the coefficient matrix. Although an attempt was made to write a program which would choose the r_k in such a manner that this would be accomplished, the program was not entirely successful. (It is conceivable that this is not even theoretically possible.) Although the method yielded the correct answers when applied to the four structure factor problem, the method failed miserably when applied to the nine structure factor diketene problem.

A program was also written which employed the Newton-Raphson method. Ideally this method should begin with a fairly good first order approximation to the desired solution, and although random signs are in general 50% correct, the method never yielded even adequate results. If the roots were not restricted to plus or minus one, a solution was obtained which yielded very small residuals, but the values of the roots bore no resemblance to the desired correct solution.

Hopefully, the information provided in this appendix will be of some value to future workers. It is regretted that the results of this work were not more encouraging.

APPENDIX B

Research Propositions

The research propositions listed below concern chemical and crystallographic questions of interest to the author which have arisen during his stay at Iowa State University. No attempt shall be made to outline a mode of experimental attack on these problems, and furthermore, it is conceivable that a thorough examination of the literature might reveal answers, or partial answers, to some of the points which are raised.

1. As mentioned in the main body of this thesis, nonlinear M-C-O groups were found in CIMH (for the iron carbonyls) and have also been reported in the literature. Although qualitative explanations have been offered, it would be interesting to see if one could predict the magnitude of the deviations of the M-C-O angles from 180° in various structures, perhaps through the use of overlap integral calculations.

2. Another natural extension from the work discussed in the main body of this thesis concerns the equivalency of the Fe-C ring distances and also the C-C ring distances in the CIMH structure. With the many improvements which have been made in the measurement of crystallographic intensity data, further refinement of the CIMH structure using more accurate data should cast considerably more light on this question. Furthermore the CIMH structure offers a distinct advantage over most other π bonded cyclopentadienyl structures in that there are two crystallographically independent molecules.

3. The presence of two crystallographically independent molecules also suggests another problem. Since the two molecules are chemically

identical, conformational or distortional differences between the two must be due entirely to their different environments. It would thus appear that this structure (possibly after further refinement) might provide the basis for studies which could reveal valuable information concerning molecular packing and potential functions.

4. The author, while reading the literature, has frequently observed that several "reputable" crystallographers do not in general correct for such things as crystal absorption or streak. An interesting problem for study thus might concern the possible systematic and random errors which result from this practice.

5. Often disorder and twinning produce similar effects on crystallographic data, and in addition it is also believed by this author that both are frequently used to "explain away" otherwise unexplainable observed phenomena and have thus become the "rug under which goodly portions of crystallographic dirt are swept." Both of these are worthy of close examination and considerable study. Concerning disorder, perhaps both crystallographic and thermodynamic techniques could be employed.

6. In 1956, Popov, Geske and Baenziger (46) reported the existence of a second crystalline modification of PCl_5 which apparently is quite stable at room temperature. Since the results of x-ray studies of the first modification are in such wide circulation (to the point at least that it is almost common knowledge that PCl_5 crystals are composed of PCl_4^+ ions and PCl_6^- ions), it is felt that a structure determination of the second modification is in order.